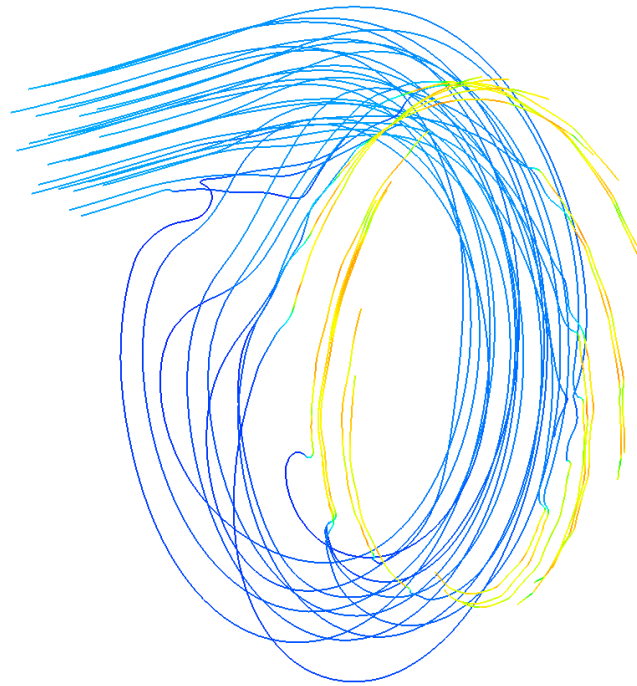




**CHALMERS**  
UNIVERSITY OF TECHNOLOGY

---



# **Method for parametrization of turbine inlet manifold for CFD-analysis**

Master's thesis in Applied Mechanics

**JOAKIM ERICSON**



MASTER'S THESIS 2016:28

# Method for parametrization of turbine inlet manifold for CFD-analysis

Joakim Ericson



Department of Applied Mechanics  
*Division of Fluid Dynamics*  
CHALMERS UNIVERSITY OF TECHNOLOGY  
Gothenburg, Sweden 2016

Method for parametrization of turbine inlet manifold for CFD-analysis  
JOAKIM ERICSON

© Joakim Ericson, 2016.

Supervisor: Ingegerd Ljungkrona, GKN Aerospace Engine System, Trollhättan Sweden

Examiner: Tomas Grönstedt, Department of Applied Mechanics

Master's Thesis 2016:28  
Department of Applied Mechanics  
Division of Fluid Mechanics  
Chalmers University of Technology  
SE-412 96 Gothenburg  
Telephone +46 31 772 1000

Cover: The streamlines of the the turbine inlet manifold.

Gothenburg, Sweden 2016

Method for parametrization of turbine inlet manifold for CFD-analysis  
JOAKIM ERICSON  
Department of Applied Mechanics  
Chalmers University of Technology

## Abstract

In this master thesis a method is developed to deal with parametric studies in order to improve evaluation of aerodynamic performance in turbine inlet manifolds for high pressure turbo pumps used in space propulsion. The main objective has been to develop a method where the analysis engineer takes control of the entire pre-process from geometry to analysis, and more independently change geometry parameters. To facilitate large parameter studies, CAD automation is implemented together with a programmed mesh script to speed up the process. A parametric study has been performed using CFD for model verification. The performance parameters studied are the impact of inlet pipe angle and percentage blocking influence in the manifold torus. The blockage has been implemented as a porous media and the performance output investigated are flow recirculation, manifold pressure loss and stator inlet condition variation. Statistical software, ModeFRONTIER, has been used to set up the test plan, and to finally analyse the results to establish correlations between input and output values. To conclude, a relatively flexible geometry model is developed using CAD-automation. To enable fully automatic mesh generation for the manifold, challenges remain. This thesis work has been done in collaboration with GKN Aerospace Engine System, within the Space Business Unit, in Trollhättan Sweden.

Keywords: Turbine inlet manifold, parametrization, CFD, CFX, ICEM, NX.



# Acknowledgements

I would like to express my greatest gratitude to my supervisor Ingegerd Ljungkrona for assistance, knowledge and expertise in aerodynamics, CFD and the turbine inlet manifold. For supporting me and contribution of his expertise in meshing techniques and hours of support in ICEM CFD, I wish to thank Lars Ljungkrona. Also Petter Johansson for his knowledge in CAD-automation and support in software. Final thanks will be given to all fellow colleagues at the department of Rotor and GKN Aerospace Engine System for letting me attend meetings, training sessions to gain knowledge of the daily life as an analysis engineer.

Joakim Ericson, Gothenburg, February 2016





# Contents

|  |             |
|--|-------------|
| <b>List of Figures</b>   | <b>xi</b>   |
| <b>List of Tables</b>  | <b>xiii</b> |
| <b>Nomenclature</b>  | <b>xv</b>   |
| <b>1 Introduction</b>  | <b>1</b>    |
| 1.1 Design of high pressure turbo pump . . . . .                                   | 1           |
| 1.2 Problem description . . . . .  | 1           |
| 1.2.1 Problems with the method used today . . . . .                                | 2           |
| 1.2.2 Technical problems of the CFD-analysis . . . . .                             | 3           |
| 1.3 Objectives and aims for this master thesis . . . . .                           | 3           |
| 1.3.1 Objectives of the method for parametric modelling . . . . .                  | 4           |
| 1.3.2 Objectives for the CFD study . . . . .                                       | 4           |
| 1.4 Limitations . . . . .  | 5           |
| <b>2 Theory</b>  | <b>7</b>    |
| 2.1 Knowledge based engineering, KBE . . . . .                                     | 7           |
| 2.1.1 Parametric modelling . . . . .   | 7           |
| 2.2 Mesh theory . . . . .  | 8           |
| 2.2.1 ICEM definitions . . . . .   | 8           |
| 2.2.2 Mesh quality . . . . .   | 8           |
| 2.2.3 Structured vs unstructured mesh . . . . .                                    | 9           |
| 2.3 Theory of compressible flow . . . . .  | 9           |
| 2.3.1 SST Turbulence model and Reynolds Averaged Navier Stoke,<br>(RANS) . . . . . | 10          |
| 2.3.2 Porous media . . . . .   | 10          |
| 2.3.3 Pressure equation . . . . .  | 10          |
| 2.4 High pressure turbo pump . . . . .   | 11          |
| 2.4.1 Physical properties of the turbine inlet manifold . . . . .                  | 11          |
| 2.4.2 Supersonic stator . . . . .  | 12          |
| 2.5 Statistical methods used . . . . .   | 13          |
| 2.5.1 Statistical Setup - Latin Hypercube . . . . .                                | 13          |
| 2.5.2 Radial basis function . . . . .  | 14          |
| 2.5.3 Multi-objective generic algorithm, MOGA II . . . . .                         | 15          |
| <b>3 Methods</b>   | <b>17</b>   |

|          |   |            |
|----------|---|------------|
| 3.1      | Method of parametrization of turbine inlet manifold . . . . .         | 17         |
| 3.1.1    | Generating the CAD-geometry model . . . . .                           | 17         |
| 3.1.2    | Automatic mesh generation - ICEM . . . . .                            | 19         |
| 3.1.3    | Existing stator mesh and extended outlet . . . . .                    | 21         |
| 3.2      | Method of CFD-analysis . . . . .                                      | 21         |
| 3.2.1    | Blocker implementation . . . . .                                      | 21         |
| 3.2.2    | CFD Computational Setup . . . . .                                     | 22         |
| 3.2.3    | Design cases setup . . . . .  | 23         |
| 3.3      | Output result parameters . . . . .                                    | 24         |
| 3.3.1    | Output of the method developed . . . . .                              | 24         |
| 3.3.2    | Output from the CFD-study . . . . .                                   | 24         |
| <b>4</b> | <b>Results</b>  | <b>27</b>  |
| 4.1      | Procedures for parametric model . . . . .                             | 27         |
| 4.1.1    | Automatic Script generation for ICEM mesh . . . . .                   | 28         |
| 4.1.2    | Result of mesh quality . . . . .                                      | 29         |
| 4.2      | Results of the parametric CFD study . . . . .                         | 30         |
| 4.2.1    | Mass flow recirculation rate and pressure loss . . . . .              | 30         |
| 4.2.2    | Manifold outlet/stator inlet . . . . .                                | 31         |
| 4.2.3    | Optimization analysis . . . . .                                       | 33         |
| <b>5</b> | <b>Discussion</b>   | <b>35</b>  |
| 5.1      | Method to facilitate parametric studies of the turbine inlet manifold | 35         |
| 5.2      | CFD analysis of the turbine inlet manifold . . . . .                  | 36         |
| <b>6</b> | <b>Conclusion</b>   | <b>37</b>  |
|          | <b>References</b>   | <b>39</b>  |
| <b>A</b> | <b>"How to manual" for generating geometries</b>                      | <b>I</b>   |
| <b>B</b> | <b>Detailed explination of the ICEM script</b>                        | <b>III</b> |
| <b>C</b> | <b>Test plan</b>  | <b>V</b>   |
| <b>D</b> | <b>Boundary condition</b>   | <b>VII</b> |
| <b>E</b> | <b>Results Massflow and static pressure into each stator segment</b>  | <b>IX</b>  |

# List of Figures

|     |  |    |
|-----|--|----|
| 1.1 | The iterative process where the CAD-engineer creates the geometry and sends it to the analysis engineer. . . . .   | 2  |
| 1.2 | The work flow today where all steps in the preprocess stage are made manually. . . . .   | 2  |
| 1.3 | Inlet conditions into the stator is desired to be uniform in circumferential direction, this means same condition in the area sections, 1,2...22,23 is desired. . . . .  | 3  |
| 1.4 | Visual definition of the parameters investigated in this report, the inlet pipe angle and recirculation area blockage. . . . .   | 3  |
| 1.5 | The analysis engineer controls the entire process, the geometry, perform meshing and do the analysis. . . . .  | 4  |
| 1.6 | The steps are made automatically by generating the CAD-geometry from an existing script. . . . .   | 4  |
| 2.1 | Visual explanation of the differences between a non-parametric and parametric approach. . . . .  | 7  |
| 2.2 | The streamline, inlet section and section 1 which measures the recirculation flow. . . . .   | 12 |
| 2.3 | Supersonic stator as Laval Nozzle between two vanes. The choking occurs in the section marked with star. [11] . . . . .  | 13 |
| 2.4 | Principles of the Latin square (bounded to 2D), the Latin Hypercube works in the same way but bounded in three dimensions. . . . .   | 14 |
| 2.5 | Principles of the Radial Basis Function - the dots are scattered data and RBFs finds the function which passes through each point. [13] . . . . .  | 14 |
| 2.6 | Principles of the multi-objective generic algorithm (MOGA II) where the objectives are to minimize T and S. The three groups of feasible, non feasible designs and the Pareto designs are shown.[14] . . . . . | 15 |
| 3.1 | The six cross sections of the geometry building the model. . . . .   | 17 |
| 3.2 | Top cross section built by the eight points defined by the radius and angle. . . . .   | 18 |
| 3.3 | The definition of the inlet pipe angle. . . . .  | 18 |
| 3.4 | The component is split into three sections, INLET, TORUS, and STATOR-InterFace part for different meshing approaches. . . . .  | 19 |
| 3.5 | The 3D-blocks which are projected to the surfaces to generate the mesh. . . . .  | 20 |

|      |  |    |
|------|--|----|
| 3.6  | Cutplane picture of the mesh shows clearly that the inlet section is made of unstructured mesh and the torus part of structured mesh. . . . .  | 20 |
| 3.7  | Capture of the mesh zoomed in to the boundary layer. . . . .   | 20 |
| 3.8  | Figure illustrates the $y^+$ value. . . . .  | 21 |
| 3.9  | Visualizing a cut plane section of the blocker. There is no flow (blocked section) through the dark grey section. Light grey illustrates where the flow passes (unblocked section). . . . .  | 22 |
| 3.10 | Overall distribution of describes the entire mesh with torus section, the stator and extended outlet. The stator is hidden with black color due to GKN proprietary information. . . . .  | 23 |
| 3.11 | The number shows the inlets to the stator between the leading edges. The first inlet section is defined at the top and the second one is the next to the right and it continues around the loop until it reaches the final 23rd. . . . . | 25 |
| 4.1  | The analysis engineer controls the entire process from geometry to analysis. . . . .   | 27 |
| 4.2  | The cross section area at the inlet section can be changed in the size or shapes. . . . .  | 28 |
| 4.3  | The inlet pipe angle can be changed in the model. . . . .  | 28 |
| 4.4  | The workflow where a master files launches several script files to generate the mesh. . . . .  | 29 |
| 4.5  | Roughly 3900 vertices are used and that the numbers are not in sequence. . . . .   | 29 |
| 4.6  | Quality of skewness and determinant of the mesh. . . . .   | 30 |
| 4.7  | Static pressure variation at the different inlets to the stator segments . . . . .   | 31 |
| 4.8  | Flow angle inlet condition into the stator around the loop. . . . .  | 32 |
| 4.9  | The performed CFD-analysis are marked squares. The dots are the virtual cases setup by ModeFRONTIER with assistance of radial basis function and MOGA II. . . . .  | 34 |

# List of Tables

|     |  |    |
|-----|--|----|
| 1.1 | Parameters of interest when investigating the design of the turbine inlet manifold [1] . . . . .   | 1  |
| 2.1 | The similarities between the geometry and ICEM . . . . .   | 8  |
| 2.2 | Two quality aspects that have been evaluated. This shows the range of the parameter and what value which satisfies the quality criteria [4] [5]. . . . .   | 8  |
| 2.3 | Differences and advantage/disadvantage of structure and unstructured mesh. [4] . . . . .   | 9  |
| 3.1 | The double if-statements which defines the blocked section. Start on top if the first condition is true, continue to the second if-condition. At the bottom the coefficients are found. Their values depended on the answers to the if-statements. . . . . | 22 |
| 3.2 | Number of elements in mesh . . . . .   | 23 |
| 3.3 | This is the test plan used. The values in bracket in the test case represents the area blocked and the inlet pipe angle respectively. . .  | 24 |
| 4.1 | Results if the parametric geometry model can handle the desired parameters or not. . . . .   | 27 |
| 4.2 | Result if mesh script can handle the parameter variation with satisfied mesh quality. . . . .  | 30 |
| 4.3 | Massflow recirculation for the test cases analyzed. . . . .  | 30 |
| 4.4 | The pressure loss coefficients for the test cases to compare and validate the analysis cases. . . . .  | 31 |
| 4.5 | Standard deviation of the flow angle for the test cases. . . . .   | 32 |
| 4.6 | Input and output values from each design case, and input information into the optimization software ModeFRONTIER. . . . .  | 33 |



# Nomenclature

|                 |  |
|-----------------|--|
| DoE             | Design of Experiments                        |
| GUI             | Graphical user interface                     |
| RBF             | Radial Basis Function                        |
| MOGA II         | Multi-objective generic algorithm            |
| $\rho$          | Density                                      |
| $\mu$           | Viscosity                                    |
| $\gamma$        | Specific heat ratio                          |
| $\delta$        | Chronicle delta                              |
| $C_{1\Delta P}$ | Total pressure loss coefficient              |
| $C_{2\Delta P}$ | Total pressure loss coefficient              |
| $C_{3\Delta P}$ | Total pressure loss coefficient              |
| $h$             | enthalpy                                     |
| $K_{loss}$      | Loss coefficient                             |
| $K_{perma}$     | Permeability coefficient                     |
| $M$             | Mach number                                  |
| $p_s$           | Static pressure                              |
| $P_T$           | Total pressure                               |
| $P_{T-in}$      | Total pressure at the inlet of the manifold  |
| $P_{T-out}$     | Total pressure at the outlet of the manifold |
| R               | Gas constant                                 |
| $q$             | Dynamic pressure                             |
| $s$             | Standard deviation                           |
| $S_m$           | Source term momentum equation                |
| $S_m$           | Source term energy equation                  |
| $U$             | Velocity                                     |
| $T$             | Temperature                                  |
| $t$             | time   |





# 1

## Introduction

This master thesis work is divided into two major categories. The first one is to develop a method of how the calculation process should be performed and the second part deals with the CFD study; hence some of the chapters and sections are split into two major parts to treat each one of them.

### 1.1 Design of high pressure turbo pump

The turbine inlet manifold is guiding the gas flow into each stator segment. It is of interest to study the aero performance of the manifold to enable new designs that are easier to manufacture. To make speed up analysis and gain more knowledge of the parameter space the method used today needs to be improved to handle more and faster analysis. This will lead to a more robust design and hopefully a less complex component to manufacture. The design process demands compromises between different disciplines e.g aero performance, solid mechanics and manufacturability. This makes the design process quite complex. The turbine inlet manifold is applicable for high pressure turbo pumps and aims to allow for a larger design space. Design parameters which is of interest to investigate is given in table 1.1

**Table 1.1:** Parameters of interest when investigating the design of the turbine inlet manifold [1]

|                                 |
|---------------------------------|
| Inlet pipe diameter             |
| Inlet pipe angle                |
| Cross section area evolution    |
| Design of blocker               |
| Stator to hub and shroud radius |

### 1.2 Problem description

This thesis work has aimed to develop a procedure of how to perform the CFD study and the problems related to that is described in the section 1.2.1. The technical problems that are related to the design of the turbine inlet manifold are describe in section 1.2.2.

### 1.2.1 Problems with the method used today

When developing turbine inlet manifolds today the CAD-engineers construct the CAD-geometry and send it to the analysis engineer to produce the mesh and perform the analysis. The geometry, mesh and analysis setup is heavily depended on each other. The mesh results and analysis outcome might demand changes of the geometry to perform the next step of analysis, therefore an iteratively process used as described in Fig 1.1.

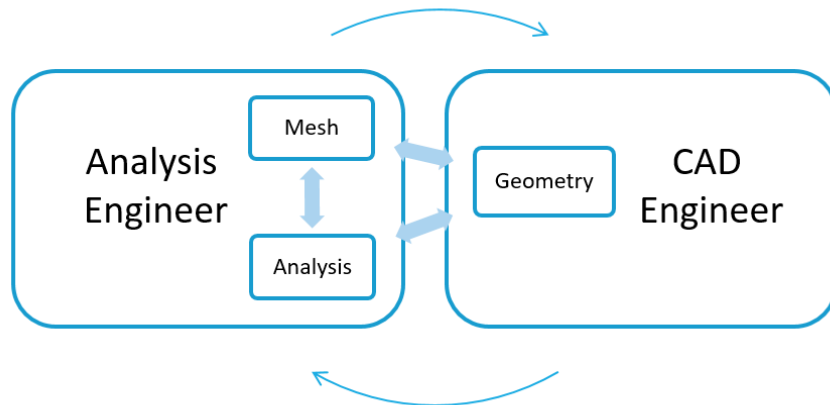


**Figure 1.1:** The iterative process where the CAD-engineer creates the geometry and sends it to the analysis engineer.

All CAD-geometries developed by the CAD-engineer need to satisfy the solid mechanics, manufacturability and aero performance design requirements. There might be conflicting interests among disciplines regarding which parameters to study, hence the ability to choose parameter independent of other disciplines is an advantage. The modelling process is very costly and time consuming. All steps are made manually as seen in 1.2 which makes it inappropriate for larger studies. To gain a robust design approach, a tool which enables quick analysis, is required. One of the challenges in this project is to parametrize the turbine inlet manifold and make it work throughout the entire process; from geometry and mesh to analysis.

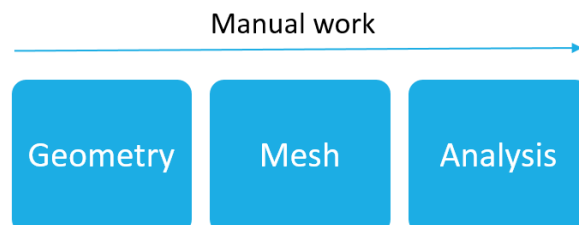


**Figure 1.2:** The work flow today where all steps in the preprocess stage are made manually.

### 1.2.2 Technical problems of the CFD-analysis

The technical optimization problems when performing the parametric study of the turbine inlet manifold performance is to reduce the pressure loss from the manifold inlet to the stator inlet. Another design criteria is to obtain similar stator inlet conditions circumferentially; i.e. similar pressure, velocity and flow angle into each stator segment to gain similar flow conditions into the rotor circumferentially. The aspect of uniformity is illustrated by figure 1.3. This study is performed to validate the design model by varying two parameters; the angle of the inlet pipe to the manifold and the blocking section to reduce flow recirculation see figure 1.4.

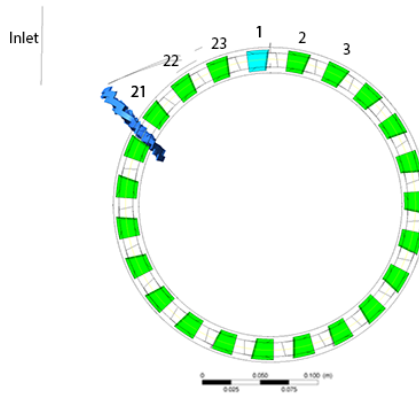


**Figure 1.3:** Inlet conditions into the stator is desired to be uniform in circumferential direction, this means same condition in the area sections, 1,2...22,23 is desired.

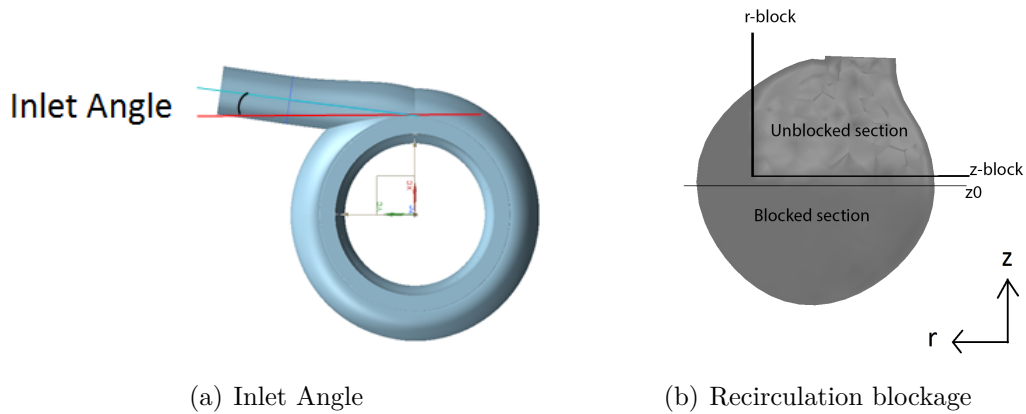


**Figure 1.4:** Visual definition of the parameters investigated in this report, the inlet pipe angle and recirculation area blockage.

## 1.3 Objectives and aims for this master thesis

The objectives and aims of this work is divided into two sections. The section, 1.3.1, describes the objectives with the developed method. The aims of the CFD-analysis is described in 1.3.2

### 1.3.1 Objectives of the method for parametric modelling

The work aims to develop a method which enable the analysis engineers to easily generate geometries and meshes based on a selected parameter variation for further studies with CFD-analysis of the turbine inlet manifold. This will enable the aero analysis engineer to more easily gain knowledge of a larger design space since the manufacturability is not included in this thesis work. This will be included in the next phase of the GKN project and therefore left for the future. The analysis engineer will have total control of the entire process, see 1.5, hence they are able to define the geometries for the parameters to study.

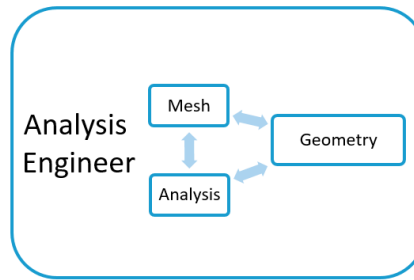


**Figure 1.5:** The analysis engineer controls the entire process, the geometry, perform meshing and do the analysis.

To facilitate large parametric studies and reduce time for the pre-process a script which handles automatical mesh generation is developed in ICEM. The entire process aims to be more automatic, where the geometry is generated by an already existing script. The work flow process aims to be as in figure 1.6. The statistical software, ModeFRONTIER, is used to set up the test plan for the parametric study.

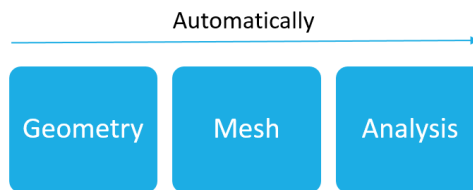


**Figure 1.6:** The steps are made automatically by generating the CAD-geometry from an existing script.

### 1.3.2 Objectives for the CFD study

The parametric study is made for model verification but also to investigate the influence of the manifold inlet pipe angle into the manifold. To reduce recirculation and hence pressure loss this thesis investigates the influence of using a blocker at the end of the loop. The results will investigate the performance with respect to, pressure-to-pressure loss between the manifold inlet and stator inlet and the standard deviation of the flow angle into the stator.

## 1.4 Limitations

This master thesis project only treats the turbine inlet manifold and the stator, deeper analysis of the flow properties downstream the stator is not made. The geometry model is used for aero performance studies, this means that the geometry in this thesis work is not made to fit analysis of solid mechanics or manufacturability. A statistical software used to set up the test plan and to analyse the output of the CFD simulations, however equations of these methods are not further investigated in this thesis work.



# 2

## Theory

This section describes the theory and the equations that have been used. This comprises an introduction to knowledge based engineering (KBE), meshing, theory of compressible flow and how to set up Design of Experiments (DoE).

### 2.1 Knowledge based engineering, KBE

Knowledge based engineering, KBE, has objectives to reduce lead-time in the product development process, by automating manual work activities. By reducing the manual work, the employees are released from their routine work and more time can be spent on new innovative solutions. One part of working with KBE system is to use parametric modelling and CAD-automation to create the geometry [2].

#### 2.1.1 Parametric modelling

In parametric modelling, the CAD model is built so all parameters are connected to each other which makes it possible to change one parameter to easily retrieve different designs. In non parametric approach the length is set to a given number while in a parametric approach the length is set to a parameter and the parameter is defined in a parameter list

Main objectives are to set up the model graphically and use expressions, in this case defined in an Excel-sheet, for the parameters that are chosen to be varied. An existing program script, updates the selected parameters and export the part-files automatically. Earlier studies has shown that the time it takes to generate CAD-models by switching from ordinary modelling methods to parametric modelling can be reduced from hours to only a few seconds [3].

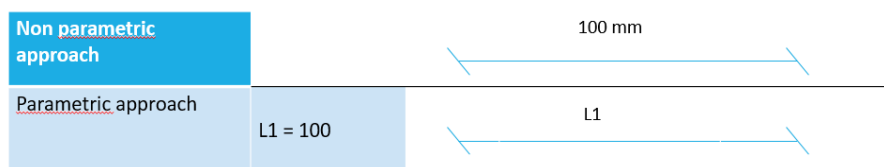


**Figure 2.1:** Visual explanation of the differences between a non-parametric and parametric approach.

To take the automization process one step further, CAD-automization can be introduced which will reduce the human action when generating a geometry model.

Advantage of this method is firstly that the geometry generation is quicker and it also makes it possible for analysis engineers without advanced knowledge of the CAD-software to generate geometries.

## 2.2 Mesh theory

This section describes theory of the mesh generation that has been used. This includes a section where scripting in ICEM is briefly introduced, a theory of mesh quality and the purpose of using structured and unstructured mesh is discussed.

### 2.2.1 ICEM definitions

The programming in ICEM is done in tcl/tk language. The approach to generate the mesh is to create blocks which will be projected to the geometrical surfaces. To understand the automatization process the definitions between the geometrical features and the ICEM blocking features needs to be explained as seen in table 2.1.

**Table 2.1:** The similarities between the geometry and ICEM

| Geometry | Block                                   |
|----------|---|
| Part     | Block -defined by six surfaces          |
| Surface  | Surface -defined by three or more edges |
| Curve    | Edge -defined by two vertices           |
| Points   | Vertex                                  |

### 2.2.2 Mesh quality

Quality of the mesh is very important which might affects the main solution. The most important numbers to check the mesh quality for a 3D-mesh is the determinant and the skewness. A negative determinant is a sign that a volume cell has a negative volume which is undesirable and the solver will not run [4]. The skewness is measure to evaluate how close to the ideal the face or the cell is. High skewness is one of the main sources of errors [5] and the accaptable value of the skewness and determinant are found in table 2.2.

**Table 2.2:** Two quality aspects that have been evaluated. This shows the range of the parameter and what value which satisfies the quality criteria [4] [5].

| Quality parameter | Range   | Acceptable value |
|-------------------|---------|------------------|
| Determinant       | -1 to 1 | >0.2             |
| Skewness          | 0 to 1  | > 0.5            |



### 2.2.3 Structured vs unstructured mesh

The two types of mesh methods used in this project are structured and unstructured meshes. A structured mesh give a higher degree for the user to control the mesh as well as an aligned grid helps the solver to converge. Some geometries are hard to make in a structured way and the time it takes more to produce a structured mesh compared to unstructured.[4]

**Table 2.3:** Differences and advantage/disadvantage of structure and unstructured mesh. [4]

|              | Structured  | Unstructured  |
|--------------|---|---|
| Advantage    | <p>Allows more user control of the mesh</p> <p>Aligned grid helps solver to converge</p>              | <p>Less effort by the user to produce mesh</p> <p>Will generate valid mesh for most of the geometries</p> |
| Disadvantage | <p>Takes more time to produce the mesh</p> <p>Some geometries might not allow structured topology</p> | <p>Harder for user to control the mesh</p>  |

## 2.3 Theory of compressible flow

The CFD problem is solved using the Navier Stokes [6] equations which generates five unknown variables,  $\rho, U, p, h, T$ . Two thermodynamic relations are therefore needed to close the set of equations.

1. Continuity equation

$$\frac{\partial \rho}{\partial t} + \nabla(\rho U) = 0 \quad (2.1)$$

2. Momentum

$$\frac{\partial(\rho U)}{\partial t} + \nabla(\rho U U) = -\nabla p + \nabla \tau + S_m \quad (2.2)$$

Where

$$\tau = \mu(\nabla U + (\nabla U)^T - \frac{2}{3}\delta \nabla U) \quad (2.3)$$

3. Energy

$$\frac{\partial(\rho h_{tot})}{\partial t} + \frac{\partial(p)}{\partial t} + \nabla(\rho U h_{tot}) = \nabla(\lambda \nabla T) + (\nabla U \tau) + U S_m + S_e \quad (2.4)$$

where  $h_{tot}$  is related to the static enthalpy by

$$h_{tot} = h + \frac{1}{2}U^2 \quad (2.5)$$

4. Equation of state for the density,  $\rho$

$$\rho = \frac{P_{tot}}{RT} \quad (2.6)$$

5. Equation of state for enthalpy  $h$

$$dh = c_p dT \quad (2.7)$$

### 2.3.1 SST Turbulence model and Reynolds Averaged Navier Stoke, (RANS)

To catch the turbulence behaviour of the flow a turbulence model must be included. The SST-model is a widely used model which combines the  $k - \epsilon$  and  $k$ -omega. The  $k - \omega$  is used in the near wall region and  $k - \epsilon$  is used in the far field flow [7]. The turbulence model also introduce averaged and fluctuating quantities which give the Reynolds averaged Navier Stokes Equation (RANS). In this turbulence model, the RANS equations are used to solve the CFD problem.

### 2.3.2 Porous media

Porous media is implemented in the momentum equation as a source to add if the permeability and a loss coefficient is desirable to be set for a defined volume [6]. When the source addition is large the momentum and flow will decrease and for an infinity large source term the momentum will be close to zero and very little will flow pass through the porous media. Hence this theory can be used a numerical approach to block flow an alternative to include a blocker element in the manifold CAD geometry. To block the flow completely through a cell, the coefficients  $C_{R1}$  and  $C_{R2}$  in equation 2.8 are set to a sufficiently large number.

$$S_{M,i} = -C_{R1}U_i - C_{R2}|U|U_i \quad (2.8)$$

### 2.3.3 Pressure equation

The total pressure for a calorically perfect gas, a gas where the change in the chemical composition is ignored, is given by

$$p_{total} = p(1 + \frac{1 + \gamma}{2}M^2)^{(\frac{\gamma}{\gamma-1})} \quad (2.9)$$

Where  $\gamma$  is the ratio of specific heats. The dynamic pressure,  $p$ , is defined in equation 2.10 where  $p_s$  is the static pressure.

$$p = \frac{1}{2}\gamma p_s M^2 \quad (2.10)$$

## 2.4 High pressure turbo pump

This section describes the theory of a high pressure turbo pump. In conjunction to this the coefficients that can be used to compare and evaluate different design cases are introduced as well as some objectives when designing a turbine inlet manifold. Introduction of the basic theory of the supersonic stator is given and the measurement of the flow angle into the stator is described.

### 2.4.1 Physical properties of the turbine inlet manifold

An optimum design of the turbine inlet manifold is a helix shaped manifold [8] but the manufacturing of such component is complex. The internal geometry is designed to produce uniform circumferential and axial flow at the stator inlet [9]. The objective when designing the manifold is to maintain the manifold outlet/stator inlet condition (static pressure, tangential velocity and mass flow) in circumferential direction. To verify and compare the test cases against each other the manifold pressure loss, recirculation rate, static pressure variation and flow angle into the stator is investigated. One method to control the pressure, velocity and flow angle into the stator is an implementation of a tongue, i.e a flow blockage, between the inlet pipe and end of volute [10].

The pressure drop coefficient  $C_{\Delta P}$  can be defined as seen in the equations below.

$$C_{1\Delta P} = \frac{P_{T-in} - P_{T-out}}{P_{T-in}} \quad (2.11)$$

$$C_{2\Delta P} = \frac{P_{T-in} - P_{T-out}}{P_{dyn-in}} \quad (2.12)$$

$$C_{3\Delta P} = \frac{P_{T-in} - P_{T-out}}{P_{dyn-out}} \quad (2.13)$$

The main stream line of the flow is shown in figure 2.2. The mass flow that passes through section 1 consist of the mass flow at the inlet and the mass flow that recirculates. The mass recirculation calculates by the equation below and the inlet and section 1 is shown in figure 2.2

$$\dot{m}_{recirculation} = \frac{\dot{m}_{section1} - \dot{m}_{inlet}}{\dot{m}_{inlet}} \quad (2.14)$$

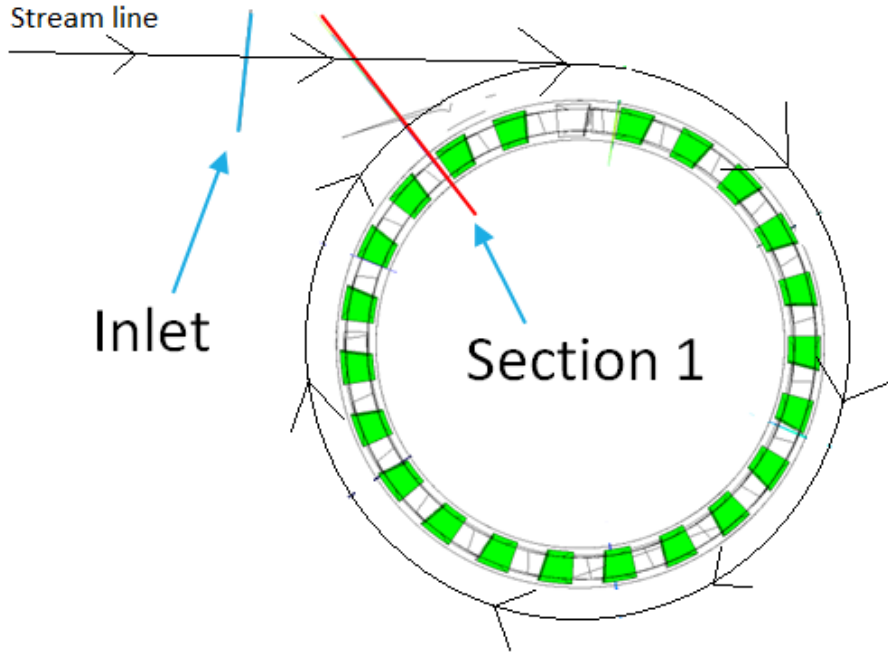


**Figure 2.2:** The streamline, inlet section and section 1 which measures the recirculation flow.

## 2.4.2 Supersonic stator

The performance of the stator is dependent on the inlet condition; pressure/Mach number and flow angle into the stator. Similar to a subsonic stator the supersonic stator is used to accelerate the fluid and direct the velocity into tangential direction. The tangential velocity component is used to turn the rotor which results in a produced torque on the pump shaft. The supersonic stator is also used as a throat and accelerates the fluid into supersonic speed. As seen in the schematic figure 2.3 the stator is as the general Laval nozzle between two vanes [11].

The flow angle into the stator is investigated and defined by the equation:

$$\alpha = \frac{v_{tangential}}{v_{axial}} \quad (2.15)$$

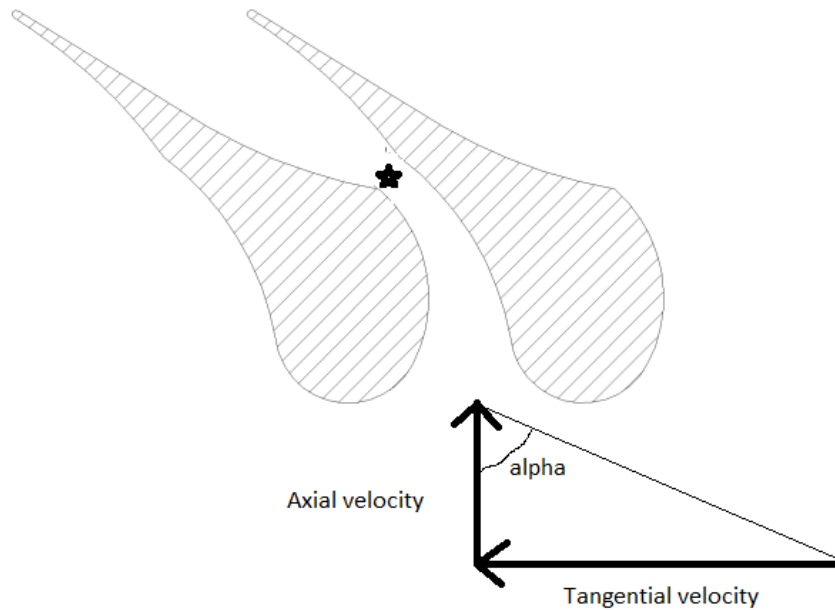


**Figure 2.3:** Supersonic stator as Laval Nozzle between two vanes. The choking occurs in the section marked with star. [11]

## 2.5 Statistical methods used

The advantage of using statistical methods is to substitute costly and time consuming experiments with mathematical models [12]. First a DoE matrix is created to efficiently generate a test plan, when the set of simulations is run and results have been extracted the statistically tool is used to find correlations between the input values and the output for the different cases. A multi-objective genetic algorithm, MOGA II, creates virtual test cases and optimizea with respect to the output values. With assistance of this the input values for the next set of test cases is found and can be analysed to improve the parametric model.

### 2.5.1 Statistical Setup - Latin Hypercube

The main objectives in computational engineering is to extract as much information as possible from the system by using as few simulations as possible. To enable this a statistical approach is to prefer. This approach reduces the number of sample points and extracts as much information of the set of analysis cases. A Latin Hypercube is a statistical method to generate samples of plausible collections in a multidimensional distribution. The Latin square is a statistical sampling divided into square grids producing a single sample point in each row and column, see figure 2.4 . The Latin hypercube is the generalized form of this and is able to deal with arbitrary and higher dimensions than the Latin square which is bounded to 2D.

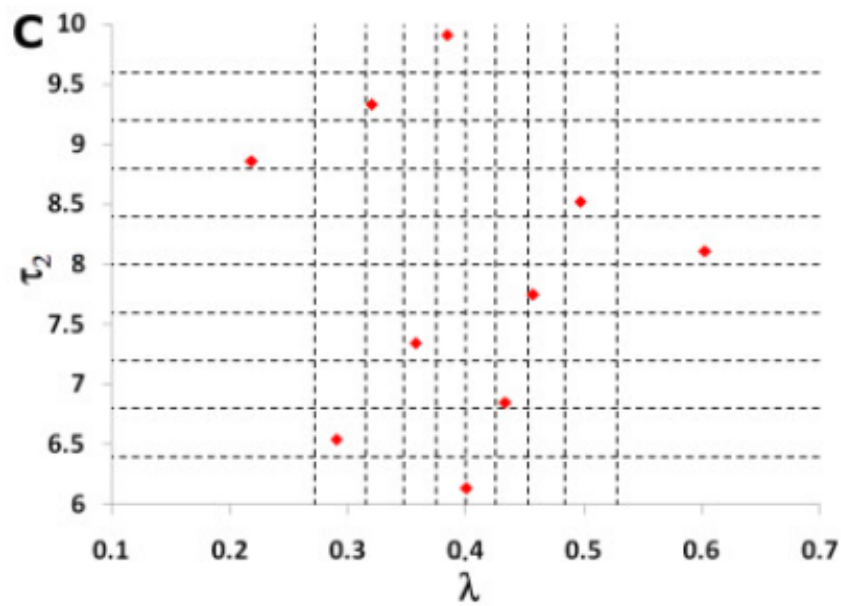


**Figure 2.4:** Principles of the Latin square (bounded to 2D), the Latin Hypercube works in the same way but bounded in three dimensions.

## 2.5.2 Radial basis function

The radial basis function is a tool which finds correlations between scattered data. The functions passes through each point of the scattered data see figure 2.5 [13].

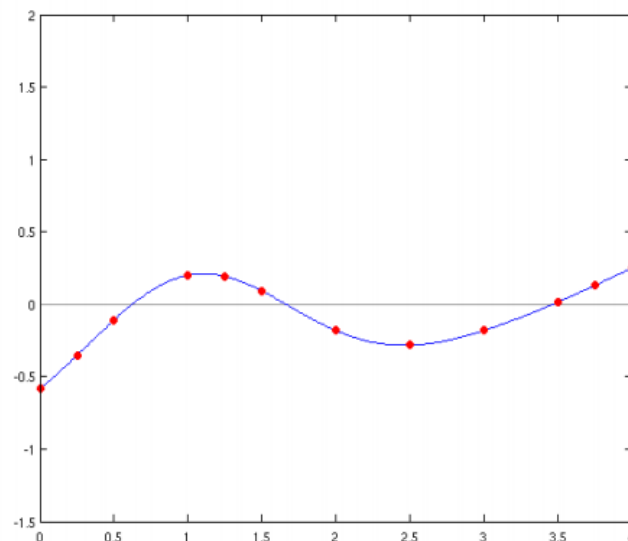


**Figure 2.5:** Principles of the Radial Basis Function - the dots are scattered data and RBFs finds the function which passes through each point. [13]

### 2.5.3 Multi-objective generic algorithm, MOGA II

The MOGA II function is used to predict the unsolved cases and generates virtual designs [12]. In a single objective algorithm, a single optimum is found; since MOGA II is a multi-objective algorithm a single optimum can not be found. Instead a set of optimum cases are found belonging to a Pareto front [14]. An example of the MOGA II is when the objectives are to minimize T and S see figure 2.6 where a certain constraint is implemented and must be satisfied. The designs are split into three groups, feasible design where all satisfies the given constraint, the unfeasible design which do not and the Pareto design which is treated as one of the optimum designs. The set of optimum designs, Pareto designs, gives the Pareto front. This gives a hint which input values that is suggested to be used for the next round of simulations to gain more knowledge of the design space.

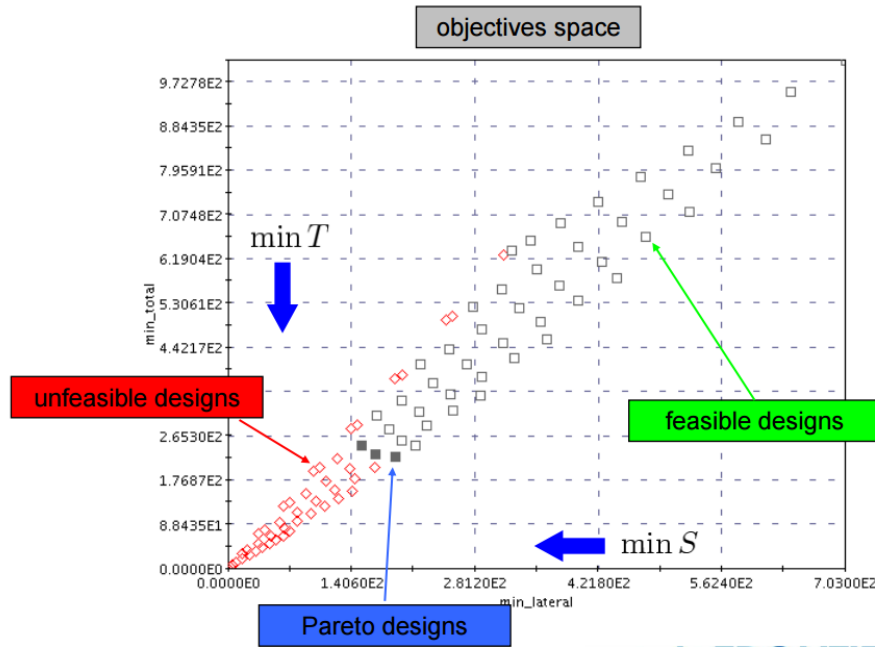


**Figure 2.6:** Principles of the multi-objective generic algorithm (MOGA II) where the objectives are to minimize T and S. The three groups of feasible, non feasible designs and the Pareto designs are shown.[14]





# 3

## Methods

All preprocess steps, geometry generation, meshing and analysis steps are heavily connected. An iterative method has therefore been used.

### 3.1 Method of parametrization of turbine inlet manifold

This subsection describes how the method for the parametrization of the manifold. This includes how the CAD-geometry is generated, the automatic mesh script developed and the stator that has been used.

#### 3.1.1 Generating the CAD-geometry model

The parameters that the model needs to deal with were shown previously in table 1.1. The geometry model is therefore developed to satisfy changes of those parameters. The model is divided into six cross sections to satisfy the constrain controlling the manifold cross section area evolution. The inlet pipe diameter is controllable at the inlet section and the stator inlet hub and shroud radius are made possible to change as well.

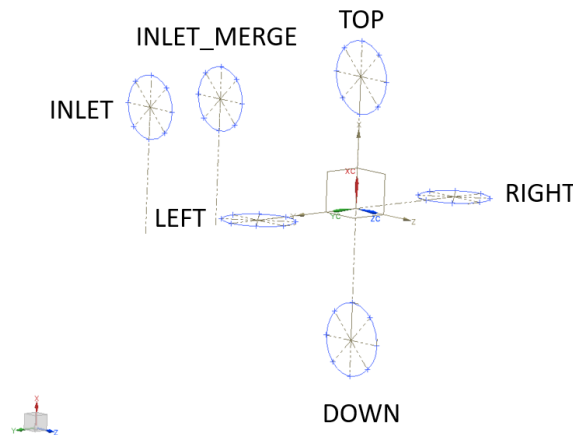


**Figure 3.1:** The six cross sections of the geometry building the model.

The points defines the radius to the local center as can be seen figure 3.2; hence the diameter/radius can be changed as a parameter at this section. The

points can be moved circumferentially around the local centre as the angle is set as a parameter. The two parameters, radius and angle, make it possible to change the cross section area shape. When the points are moved, due to varying radius or angle, the splines follow and ensure that the loop is closed to continue and create surfaces. The pipe inlet angle is also set as a parameter which has been constrained by the angle between the inlet sketch plane and the yz-reference plane.

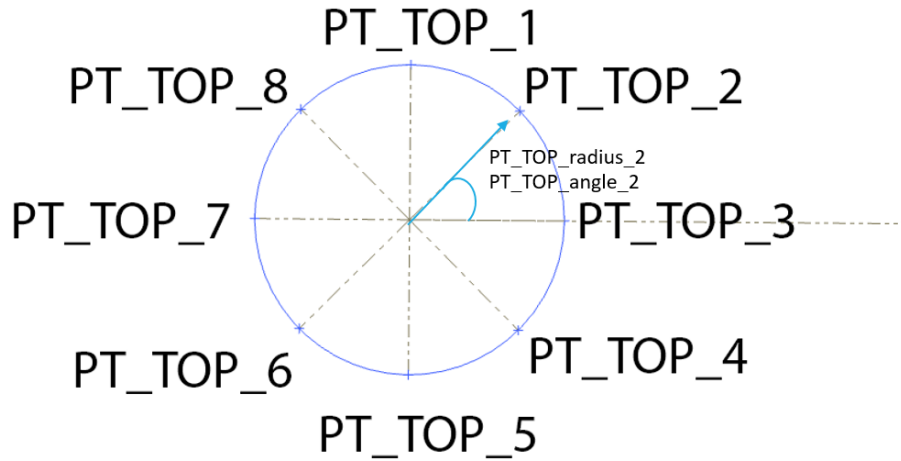


**Figure 3.2:** Top cross section built by the eight points defined by the radius and angle.

A script is used at GKN Aerospace Engine System which connects the CAD-software NX 9.0 to Microsoft Excel. Therefore all parameters and values are defined in a Microsoft Excel sheet. The pipe inlet angle is defined in figure 3.3.

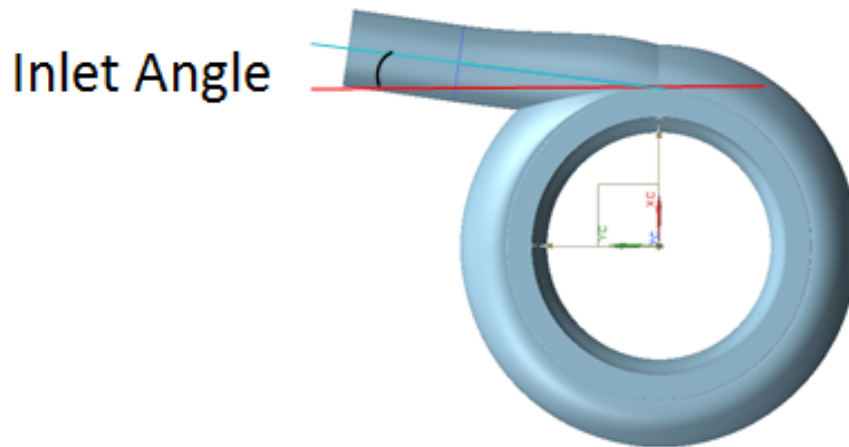


**Figure 3.3:** The definition of the inlet pipe angle.

### 3.1.2 Automatic mesh generation - ICEM

The geometry model is divided into three parts and named according to figure 3.4. The INLET-PART will be meshed as an unstructured mesh with prism cells, as the geometry makes it hard to generate a structured mesh for this part. The TORUS- and STATOR Interface part is created as a structured mesh.

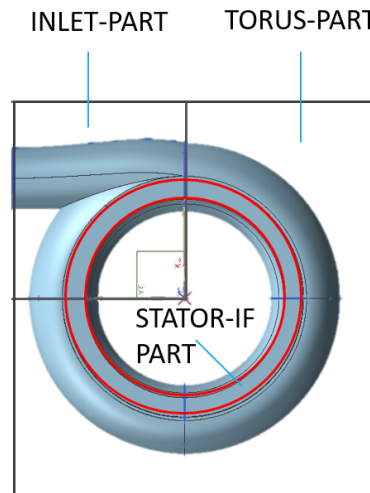


**Figure 3.4:** The component is split into three sections, INLET, TORUS, and STATOR-InterFace part for different meshing approaches.

To deal with the large number of cases an automatic mesh generation script has been developed using ICEM CFD v.16.

The script handles the following steps in order to create the mesh:

1. Import the CAD-model into ICEM
2. Generate blocks 2D - surface blocks
3. Creating 2D-surface mesh and check mesh quality
4. Converting 2D - blocks into 3D
5. Create O-Grid around wall surfaces
6. Generate 3D-mesh - check quality
7. Define sub-domain for the re-circulation block (will be defined as porous media)

The 3D-blocks are projected to the geometrical surface and create the mesh as can be seen in figure 3.5, showing the surface mesh. The final volume mesh is a combination of a structured and an unstructured mesh which becomes easy to see when a cutplane picture is taken as illustrated in figure 3.6.

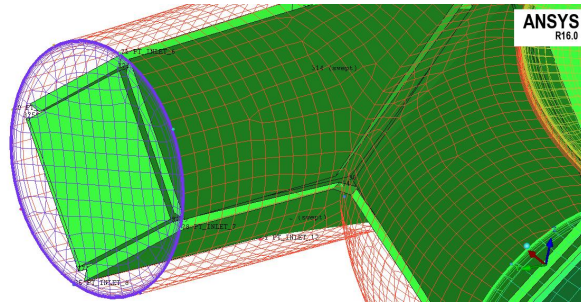


**Figure 3.5:** The 3D-blocks which are projected to the surfaces to generate the mesh.

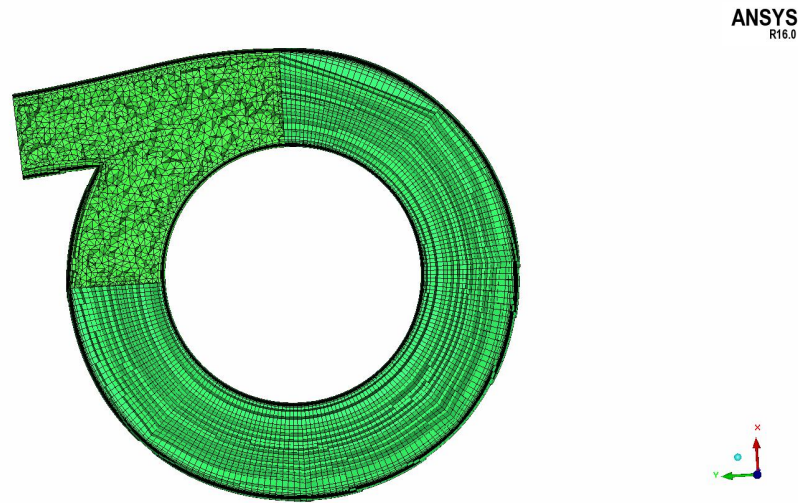


**Figure 3.6:** Cutplane picture of the mesh shows clearly that the inlet section is made of unstructured mesh and the torus part of structured mesh.

To capture the boundary layer flow, a boundary layer mesh is implemented close to the wall. This can be seen in figure 3.7 where the elements close to the wall are much smaller. The resolution of the boundary layer is describe by  $y^+$  which is roughly 20 and can be seen in figure 3.8.

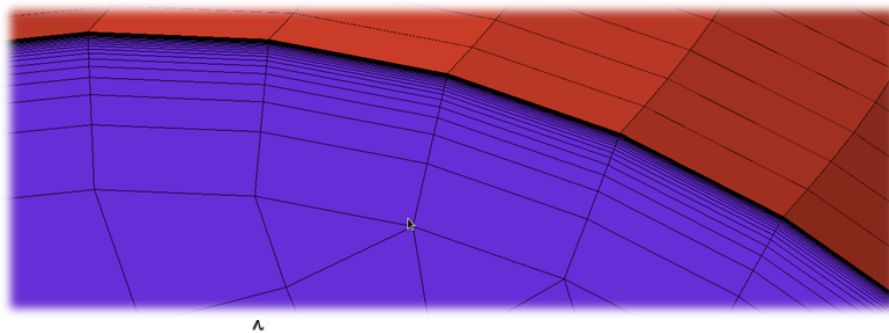


**Figure 3.7:** Capture of the mesh zoomed in to the boundary layer.

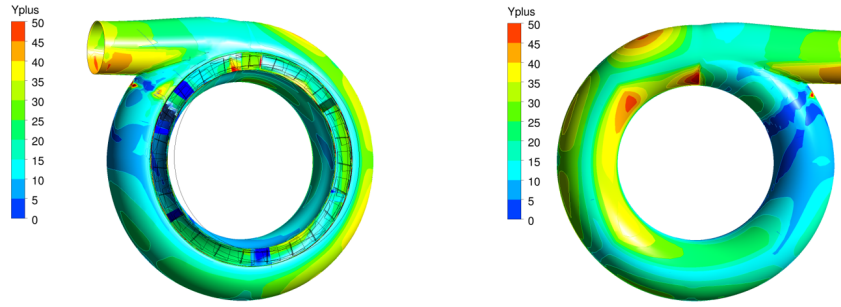


**Figure 3.8:** Figure illustrates the  $y^+$  value.

### 3.1.3 Existing stator mesh and extended outlet

The main objective is to evaluate the performance of the manifold. To do this a general stator model needs to be included to give the flow resistance from the stator leading edges as well as realistic working conditions. The stator used in this project is not subject to change since it has been used in a previous GKN project. Since this master thesis only investigates the manifold, the rotor is not taken into account and an extended outlet is modelled downstream the stator to improve stability and convergence.

## 3.2 Method of CFD-analysis

This section describes the method used to perform the CFD-analysis. Description of the test plan setup and the statistical evaluation is also given.

### 3.2.1 Blocker implementation

The blocking sections are created by letting all volume cells in the cut-plane shown in figure 3.9 be treated as a sub-domain and be given properties as porous media. The blocking section is located just before the torus part and connecting the inlet pipe part which is shown in figure 3.9. This is a simplification and a faster method compared to creating a blocker in the geometry model. The amount of blocked area is used as a parameter as is varied for the different test cases. The definition of the blocked area is described according to the double if statements in table 3.1; the coefficients  $C_{R1}$  and  $C_{R2}$  affect the momentum source equation 2.8. The coefficients are set to a large number, in this case  $10^7$  in the area to be blocked and to 0 at the non blocked area. This can be seen in figure 3.9, the lower and the left side is dark grey which is blocked and the light grey is unblocked. Since z-block and r-block will vary according to the test table the blocked area will vary among the test cases.

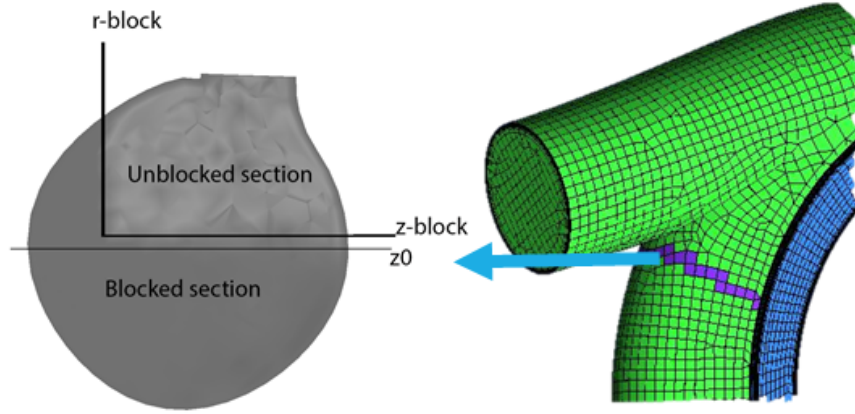


**Figure 3.9:** Visualizing a cut plane section of the blocker. There is no flow (blocked section) through the dark grey section. Light grey illustrates where the flow passes (unblocked section).

**Table 3.1:** The double if-statements which defines the blocked section. Start on top if the first condition is true, continue to the second if-condition. At the bottom the coefficients are found. Their values depended on the answers to the if-statements.

| if ( $r < r\text{-block}$ ) |                 |                 |
|-----------------------------|-----------------|-----------------|
| True                        |                 | False           |
| if ( $z < z\text{-block}$ ) |                 |                 |
| True                        | False           |                 |
| $C_{R1} = 0$                | $C_{R1} = 10^7$ | $C_{R1} = 10^7$ |
| $C_{R2} = 0$                | $C_{R2} = 10^7$ | $C_{R2} = 10^7$ |

### 3.2.2 CFD Computational Setup

The Ansys CFX v.16 software was used to perform the CFD-analysis. The steady state analysis for compressible flow is solved together with the SST turbulence model. The boundary condition at the inlet set as a total temperature condition and a total and static pressure condition is given at the outlet. Values of the boundary conditions is found in Appendix D. The CFD model is plotted in figure 3.10 which also shows the entire mesh, with the stator mesh hidden due to GKN proprietary information. In table 3.2, the number of the different cell types are shown. Wall conditions for the torus part is set to non-slip but for the stator ring and extended outlet a slip wall condition is used. This is because the stator mesh has no refinements for the boundary layer. The fluid is a gas mixture of oxygen and hydrogen.

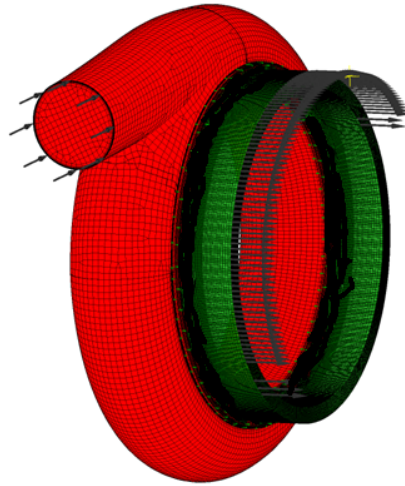


**Figure 3.10:** Overall distribution of describes the entire mesh with torus section, the stator and extended outlet. The stator is hidden with black color due to GKN proprietary information.

**Table 3.2:** Number of elements in mesh

| The types of elements | Number of elements |
|-----------------------|--------------------|
| Tetra                 | 85000              |
| Hexa                  | 400000             |
| Tri                   | 200                |
| Penta                 | 8300               |
| Quad                  | 4300               |
| Pyra                  | 4000               |

### 3.2.3 Design cases setup

To make the parametric study more efficient the Latin hypercube method was used. This is done to maximize the knowledge of the design space for the least number of design cases evaluated. The parametric values to be varied are defined in the list below

1. Inlet angle
2. Block in r-direction
3. Block in z-direction

Since the values of the blocking in radial direction and in axial-direction (z-direction) give the total blocking. This values are stated in the parametric table below 3.3. The name of test cases are defined in sequence from 0 to 10.

**Table 3.3:** This is the test plan used. The values in bracket in the test case represents the area blocked and the inlet pipe angle respectively.

| Test Case     | Area blocked | Inlet Angle |
|---------------|--------------|-------------|
| 7 ( 1 , -5 )  | 1            | -4,7        |
| 10 ( 14 , 8 ) | 14           | 8,1         |
| 9 ( 20 , 8 )  | 20           | 8,1         |
| 6 ( 25 , -4 ) | 25           | -3,7        |
| 5 ( 40 , 8 )  | 40           | 8,1         |
| 0 ( 41 , -2 ) | 51           | -1,5        |
| 1 ( 56 , 0 )  | 56           | -0,4        |
| 4 ( 63 , -9 ) | 63           | -8,8        |
| 8 ( 78 , 1 )  | 78           | 1,0         |
| 2 ( 78 , 3 )  | 78           | 3,0         |
| 3 ( 93 , 2 )  | 93           | 2,4         |

### 3.3 Output result parameters

This section summaries the outputs and results that are expected from the method developed and the CFD-study performed.

#### 3.3.1 Output of the method developed

Deliverables for the method developed is to show how far the automatization process has reached. The parametric model is given together with the Excel-sheet to be used to produce future geometries. The results of the mesh-script programming is also given.

#### 3.3.2 Output from the CFD-study

Output of the simulations are the total pressure loss between the inlet and the manifold outlet, static pressure and flow angle into each stator section circumferentially. This will show how the manifold design parameters influences the performance. Mass flow at the inlet and inflow sections around the manifold will be measured. This will be done to investigate the recirculation rate in the manifold for different cases. The static pressure around the loop and the flow angle are examined since this affects



the performance of the stator and later the rotor and the overall performance as said previously. The main criteria to be observed are thus:

1. Massflow and mass recirculation
2. Static pressure at each stator inlet segment
3. Flow angle at each stator inlet segment

The recirculation of the mass flow is defined as described in the theory part, section 1 and the inlet is shown in figure 3.10. To examine the variations of the inlet conditions in to the stator around the loop each inlet section is named from 1-23. The section on top is number one and the next to the right is number two and so it continues around the loop as seen in figure 3.11. This is applicable to evaluate the static pressure and flow angle into the stator segment.

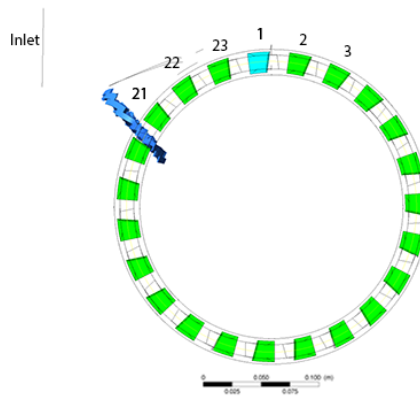


**Figure 3.11:** The number shows the inlets to the stator between the leading edges. The first inlet section is defined at the top and the second one is the next to the right and it continues around the loop until it reaches the final 23rd.



# 4

## Results

This chapter shows the results of this project. This section is divided into two main parts where the first one gives results of the method developed and the second section shows the results of the CFD-analysis.

### 4.1 Procedures for parametric model

The method developed in this work enables the the analysis engineers to control the entire process from geometry generation, mesh to analysis input as seen from figure 4.1. The iterative work is faster since the analysis engineer does not need to include a design engineer to create the geometry. No previous knowledge of NX or the CAD-software is needed since the geometry is controlled by geometry parameters in the Microsoft Excel-sheet and an existing script is launched in the Windows command terminal to generate the geometries. The geometry model can handle variation for all parameters of interest without failing as seen in table 4.1.

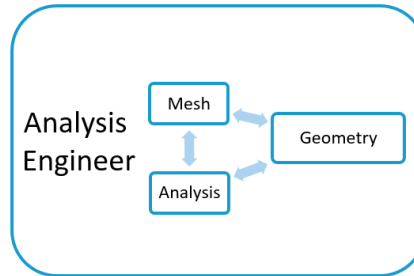


**Figure 4.1:** The analysis engineer controls the entire process from geometry to analysis.

**Table 4.1:** Results if the parametric geometry model can handle the desired parameters or not.

| Parameter                       | Results         |
|---------------------------------|-----------------|
| Inlet pipe diameter             | OK              |
| Inlet pipe angle                | OK              |
| Cross section area evolution    | OK              |
| Design of blocker               | Not implemented |
| Stator to hub and shroud radius | OK              |

Results of variation of the inlet section area are shown in figure 4.2 and is an example of how each cross section can be varied. As seen, the inlet area can be decreased uniformly for all points and maintain the circular shape or be decreased in just some desired points as seen in the right of figure 4.2. Results of different pipe inlet angle are shown in figure 4.3.

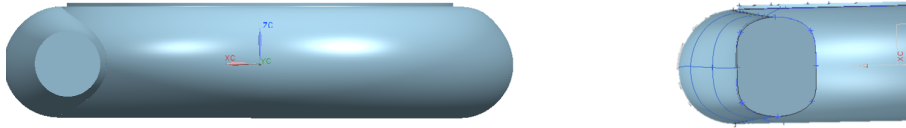


**Figure 4.2:** The cross section area at the inlet section can be changed in the size or shapes.

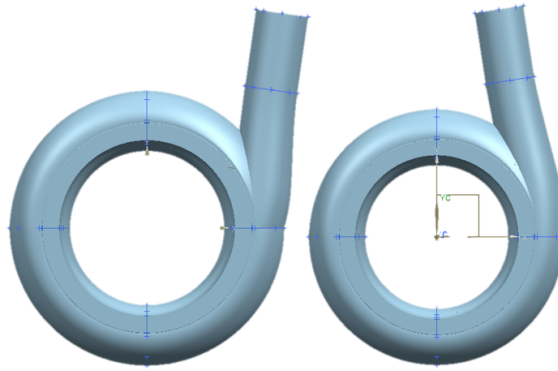


**Figure 4.3:** The inlet pipe angle can be changed in the model.

### 4.1.1 Automatic Script generation for ICEM mesh

An automatic script has been developed to generate meshes quickly. A master file calls sub-files to perform the meshing. This makes it possible to work with one test case and when the meshing is completed the master file continues to the next test case performing the mesh. The master file is built by a for-loop where it is looped over the test cases so the mesh can be produced for all the test cases by launching the master file once. The work flow of the script is described in figure 4.4. An advantage of splitting the script into sub-files is that if one script is failing it is possible to run the script prior to it and produce the failing script manually and then launch the scripts next in the chain.

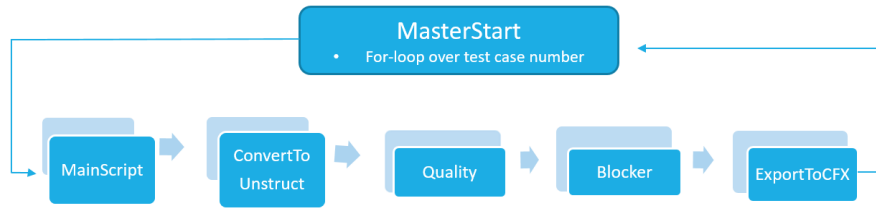


**Figure 4.4:** The workflow where a master files launches several script files to generate the mesh.

There are some challenges that arise with ICEM and the scripting procedures. As described in section 2.2 the programming is defined by the vertex number and since these are set by ICEM, huge challenge rises when making automated mesh. If the geometry is changed or adjusted, the vertex number might change which results in that an edge is associated to wrong curve. Figure 4.5 shows the vertex are highly unsequenced and roughly 3900 vertices's are used to program and mesh this component. A result of this might be that the entire program crashes and ICEM needs to be restarted or the mesh script runs and produces a mesh that does not satisfy the mesh quality criteria.

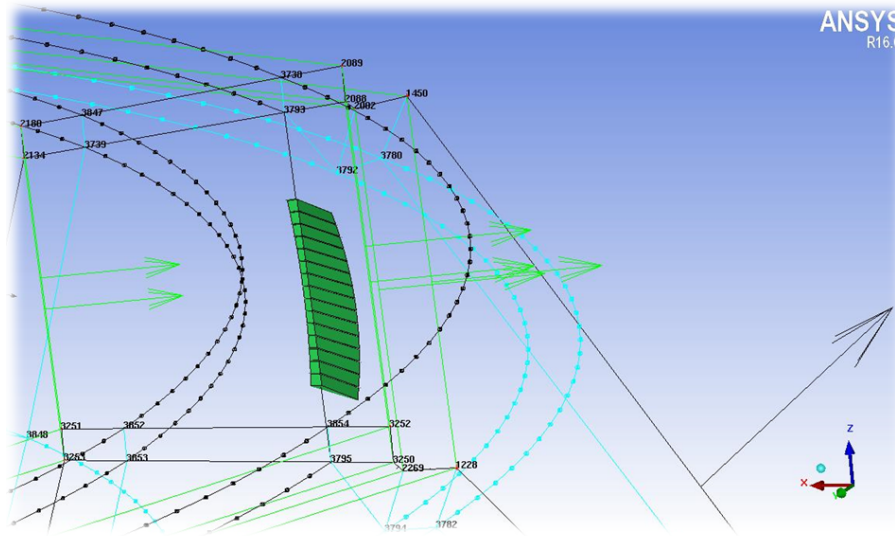


**Figure 4.5:** Roughly 3900 vertices are used and that the numbers are not in sequence.

#### 4.1.2 Result of mesh quality

The mesh quality is one of the main issues in this project. For cases that were run for CFD-analysis, the mesh quality was satisfied the by criteria given in 4.2. The quality of the determinant is poor as can be seen in figure 4.6a and the skewness is poor but runnable. The problem in the meshing step is to satisfy the mesh quality independent of the parameter variation. This scripts only work with variation in the inlet pipe angle and percentage area blocked in the blocked section. The results of the mesh quality with respect of each parameter is given in table 4.2.

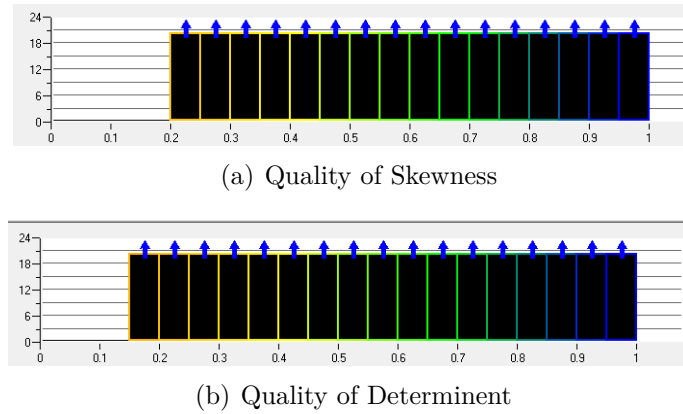


**Figure 4.6:** Quality of skewness and determinant of the mesh.

**Table 4.2:** Result if mesh script can handle the parameter variation with satisfied mesh quality.

| Parameter                       | Results |
|---------------------------------|---------|
| Inlet pipe diameter             | NOT OK  |
| Inlet pipe angle                | OK      |
| Cross section area evolution    | NOT OK  |
| Design of blocker               | OK      |
| Stator to hub and shroud radius | NOT OK  |

## 4.2 Results of the parametric CFD study

This section gives the results of the CFD-analysis and a comparison between the different test cases. Exact values of the results are shown in Appendix E.

### 4.2.1 Mass flow recirculation rate and pressure loss

The recirculation for the test cases are shown in table 4.3. Results indicate that an increased area blockage results in a decreased mass flow recirculation in most of the cases. However, this is not applicable to test case 5 and 6 which show that the case 5 has a higher recirculation rate than the test case 5. The fact gives a hint that the pipe inlet angle affects the flow recirculation. The mass flow in the system are shown in Appendix E.

The pressure loss between the inlet and the stator inlet for the different test cases are shown in 4.4. The results show that the pressure loss are decreasing until a percentage area blocking range at around 56-78 % where the pressure loss increases again.

**Table 4.3:** Massflow recirculation for the test cases analyzed.

| Test Case   | Area blocked % | Flow re-circulation % |
|-------------|----------------|-----------------------|
| 7 ( 1, -5)  | 1              | 92                    |
| 10 ( 14, 8) | 14             | 81                    |
| 9 ( 20, 8)  | 20             | 71                    |
| 6 ( 25, -4) | 25             | 43                    |
| 5 ( 40, 8 ) | 40             | 47                    |
| 0 ( 51, -2) | 51             | 34                    |
| 1 ( 56, 0 ) | 56             | 32                    |
| 4 ( 63, -9) | 63             | 24                    |
| 8 ( 78, 1)  | 78             | 12                    |
| 2 ( 78, 3)  | 78             | 13                    |
| 3 ( 93, 2)  | 93             | 0                     |

**Table 4.4:** The pressure loss coefficients for the test cases to compare and validate the analysis cases.

| Test Case     | Area blocked<br>% | $\Delta P / P_{INLET}$<br>% | $\Delta P / P_{dynINLET}$<br>% |
|---------------|-------------------|-----------------------------|--------------------------------|
| 7 ( 1 , -5 )  | 1                 | 2,0                         | 48,9                           |
| 10 ( 14 , 8 ) | 14                | 1,9                         | 45,9                           |
| 9 ( 20 , 8 )  | 20                | 1,8                         | 43,6                           |
| 6 ( 25 , -4 ) | 25                | 2,1                         | 51,7                           |
| 5 ( 40 , 8 )  | 40                | 1,1                         | 27,2                           |
| 0 ( 51 , -2 ) | 51                | 1,0                         | 25,3                           |
| 1 ( 56 , 0 )  | 56                | 0,9                         | 23,2                           |
| 4 ( 63 , -9 ) | 63                | 0,9                         | 22,7                           |
| 8 ( 78 , 1 )  | 78                | 0,8                         | 19,6                           |
| 2 ( 78 , 3 )  | 78                | 1,4                         | 35,7                           |
| 3 ( 93 , 2 )  | 93                | 1,4                         | 36,8                           |

#### 4.2.2 Manifold outlet/stator inlet

The static pressure into each stator segment is plotted in Figure 4.7. In the circumferential direction, the section 1,2..22,23 describe where the flow enters the stator. The static pressure is shown in radial direction where the pressure is increased with the radius. A figure with the static pressure values is shown in Appendix E. As seen the static pressure is decreasing around the 17-18th leading edge which leads to an increased velocity; the velocity increases as the percentage of the blocking decreases. The blocking affects the flow upstream.

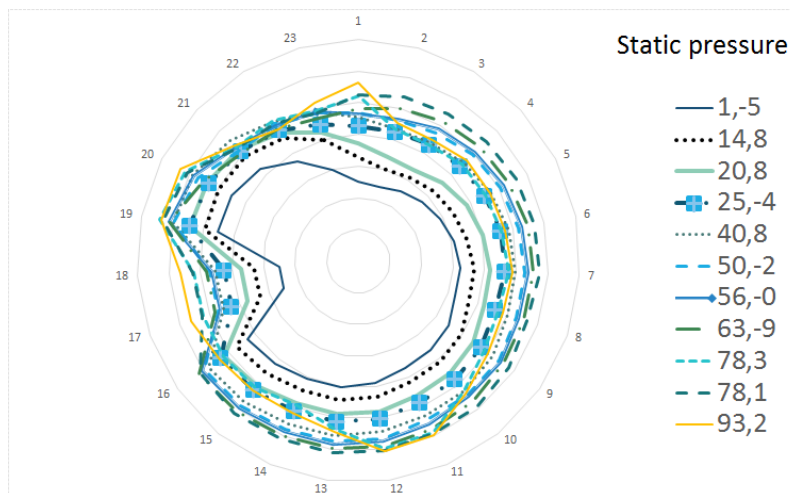


**Figure 4.7:** Static pressure variation at the different inlets to the stator segments

The flow angle into the leading edges in the stator around the loop are shown in figure 4.8. In circumferential direction the different sections between the leading edges are explained and the flow angle is given in the radial direction where the angle is increasing with increasing radius. The standard deviation for the inlet angle is

given in 4.5. The less the flow is blocked the less is the STD of the flow angle into the stator. The reason for this is probably due to the blockage that disturbs the main flow and creates a less well behaved flow distribution.

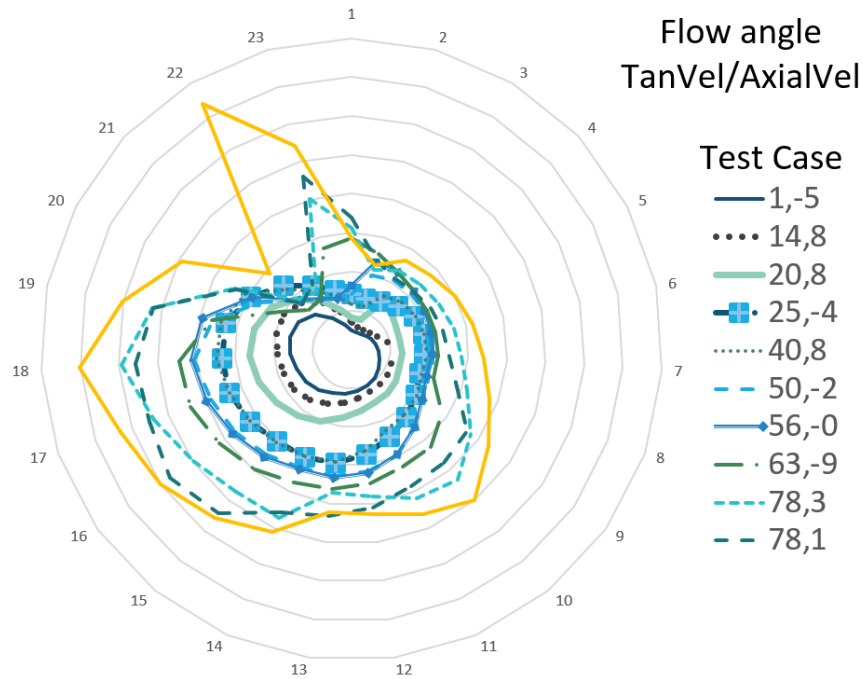


**Figure 4.8:** Flow angle inlet condition into the stator around the loop.

**Table 4.5:** Standard deviation of the flow angle for the test cases.

| Test Case     | Area blocked % | STD Angle |
|---------------|----------------|-----------|
| 7 ( 1 , -5 )  | 1              | 3,96      |
| 10 ( 14 , 8 ) | 14             | 4,64      |
| 9 ( 20 , 8 )  | 20             | 5,49      |
| 6 ( 25 , -4 ) | 25             | 6,90      |
| 5 ( 40 , 8 )  | 40             | 7,33      |
| 0 ( 51 , -2 ) | 51             | 8,24      |
| 1 ( 56 , 0 )  | 56             | 8,43      |
| 4 ( 63 , -9 ) | 63             | 8,85      |
| 8 ( 78 , 1 )  | 78             | 13,10     |
| 2 ( 78 , 3 )  | 78             | 11,94     |
| 3 ( 93 , 2 )  | 93             | 14,74     |



### 4.2.3 Optimization analysis

Input to the evolutionary algorithm tool, which includes the input and output of the CFD analysis are listed in figure 4.6. The third, ninth and tenth column are input values to the CFD analysis and fourth to the eighth are output from the CFD analysis.

| Test Case     | Area blocked | Pipe Inlet Angle | Re-circulation Blocking | $\Delta P / P_{INLET}$ | $\Delta P / P_{dynINLET}$ | STD Angle | Max - min | r-block | z-block |
|---------------|--------------|------------------|-------------------------|------------------------|---------------------------|-----------|-----------|---------|---------|
| 7 ( 1 , -5 )  | 1            | -2               | 92                      | 2,0                    | 48,9                      | 4         | 34        | -8      | 153     |
| 10 ( 14 , 8 ) | 14           | 0                | 81                      | 1,9                    | 45,9                      | 5         | 28        | 1       | 160     |
| 9 ( 20 , 8 )  | 20           | 3                | 71                      | 1,8                    | 43,6                      | 5         | 42        | 18      | 156     |
| 6 ( 25 , -4 ) | 25           | 2                | 43                      | 2,1                    | 51,7                      | 7         | 51        | 32      | 164     |
| 5 ( 40 , 8 )  | 40           | -9               | 47                      | 1,1                    | 27,2                      | 7         | 29        | 8       | 166     |
| 0 ( 51 , -2 ) | 51           | 8                | 34                      | 1,0                    | 25,3                      | 8         | 23        | -17     | 153     |
| 1 ( 56 , 0 )  | 56           | -4               | 32                      | 0,9                    | 23,2                      | 8         | 20        | -23     | 158     |
| 4 ( 63 , -9 ) | 63           | -5               | 24                      | 0,9                    | 22,7                      | 9         | 12        | -35     | 169     |
| 8 ( 78 , 1 )  | 78           | 1                | 12                      | 0,8                    | 19,6                      | 13        | 40        | 20      | 163     |
| 2 ( 78 , 3 )  | 78           | 8                | 13                      | 1,4                    | 35,7                      | 12        | 18        | -22     | 167     |
| 3 ( 93 , 2 )  | 93           | 8                | 0                       | 1,4                    | 36,8                      | 15        | 14        | -30     | 167     |

**Table 4.6:** Input and output values from each design case, and input information into the optimization software ModeFRONTIER.

It is of interest to minimize the pressure drop and also the standard deviation of flow angle into the stator. When all cases are optimized for these two objectives, a Pareto front is found as shown in figure 4.9. The numbered squares are results from the CFD analysis and the black dots are virtual cases defined by the statistical method. An interesting results is that there is a point around case 0,3 and 4 where the pressure drop is at its lowest value and start to increase if the area blockage is further increased as for case 2, 8 and 1.

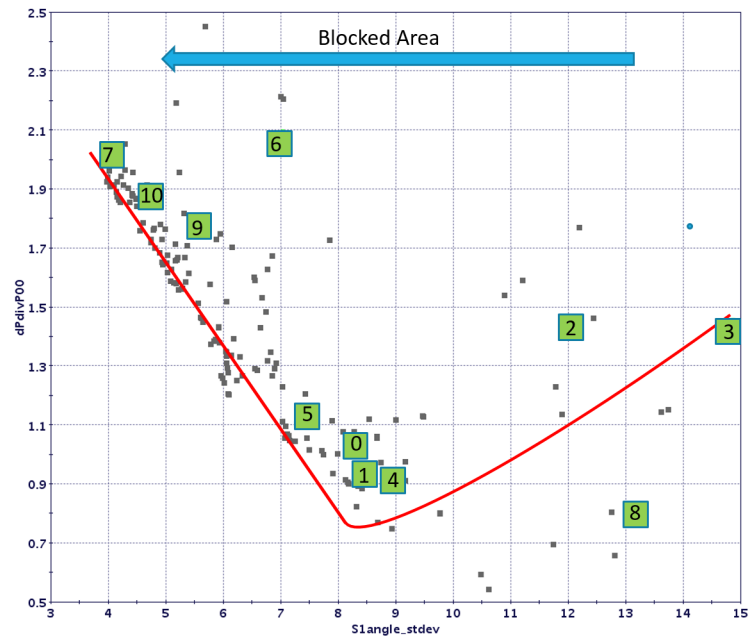


**Figure 4.9:** The performed CFD-analysis are marked squares. The dots are the virtual cases setup by ModeFRONTIER with assistance of radial basis function and MOGA II.

# 5

## Discussion

The first part of this section discusses the method that has been developed to perform parametric studies of the turbine inlet manifold. The second section analyses the results of the performed CFD analysis.

### 5.1 Method to facilitate parametric studies of the turbine inlet manifold

The method developed has increased the degree of automation for parametric studies of the turbine inlet manifold. This process is comprehensive in smaller scale parametric studies with less than 30 cases. Since theory states that over 100 or even 1000 design cases are needed for statistically proven results, this method needs to be refined and more automatic methods implemented. This is due to the manual work that is demanded for each case. One of the main advantage with this method and a results of this thesis work is that engineers without or with only limited knowledge of the CAD-tool NX are able to efficiently create new geometries for analysis.

Implementing support lines in the CAD-geometry could be one possible solution to ensure same mesh quality independent of the geometry dimension. This will however lead to further problems with the meshing such as a more complex geometry. There is a problem to import lines into ICEM from NX. ICEM seems to support this feature but error message occurs when trying use this method. When the O-Grid is generated, all block edges are generated in the same step hence the name of each vertex and edge is randomly labelled. This has been observed when the pipe inlet angle changes. In some cases the block edge names have been changed since the geometry is changed; this step seems hard to do automatically. One way to work around this problem is to write a master file which opens each file and launches desired the script files and saves the project before a manual quality check. It is also preferable recommended to evaluate other mesh software than ICEM, to see if other program's can handle automatic mesh-generation in a better way. The way that ICEM handles scripting works really good if the purpose is to mesh the exact same geometries many times, but when parameters are changed and the geometries are not identical the mesh software gives problems. This is observed as poor mesh quality or a total crash of the software which lead to a restart of the program. This is the main outcome of this project in terms of the mesh-generation. GKN Aerospace has decided to evaluate other mesh software to perform automatic meshing for complex parametric models.

Porous media can be used as a blocking section in the early concept phase to handle quick analysis of different blockage types. When the final design should be analyzed a geometrical blocking should be implemented to treat wall behaviour more accurately since there is no wall function connected to the porous media. For further investigation of the blockage type some suggestions are made to redirect the blockage more into the stream direction.

### 5.2 CFD analysis of the turbine inlet manifold

The parametric study results show that the blocking and pipe inlet angle influence the performance. The study performed is too small to draw any statistically proven conclusion but in figure 4.9 it is interesting to see the Pareto front and the tendency that at a certain percent of blockage, the pressure loss starts to increase even more. The results here are only based on the turbine inlet manifold and no attempts have been taken for the overall turbine performance. This must be done to make any further conclusion of the manifold design. There would be interesting to investigate the outlet condition of the stator, if the standard deviation of the flow angle give some effects downstream or if the stator can handle this variation. This study was performed with few test cases due to the time constrain. To gain a statistically proven results of the study, more test cases are recommended to be performed. This means more cases where the two parameters, pipe inlet angle and percentage area blockage are evaluate or a larger parametric study could include all parameters in table 1.1.

The static pressure drop between stator segment 17 and 18 probably occurs because of the high recirculation of the mass flow in the manifold. The reason for this could be higher mass in the manifold when the blockage is decreased. This would lead to an acceleration of the main flow. The main reason for the pressure drop between the manifold inlet and manifold outlet is the friction at the wall since this is an internal flow. This is one of the reasons why the flow is supposed to exit to the stator during the first loop.

# 6

## Conclusion

The ability to make a geometric parametric model of the turbine inlet manifold has been proven. The challenges of this method is to have the overview perspective in all steps and make all steps work together for different kinds of design cases. Suggestions to evaluate if other meshing tools than ICEM can be used to generate the mesh are suggested, since programming complex mesh automation in ICEM seems hard. Other thoughts might be to use ICEM but divide the part into several meshes and merge them together in CFX or in the end of an ICEM session. A parametric study proved that the method worked for a smaller scale study and the outcome of the study would be to investigate the influence of the flow downstream the stator and see if the system can handle variations at the stator inlet.



# List of References

- [1] GKN Aerospace Enginge System (2015) Master thesis proposal ,GKN Aerospace Engine System (2015) .
- [2] Sandberg,M. (2003) Knowledge based engineering - In Product Development, Luleå University of Technology, ISSN: 1420-1536
- [3] Chen , X. Zheng, H. Gang, P. Ji, X. (2014) PARAMETRIC MODELLING SYSTEM OF GAS TURBINE COMBUSTOR . Technical Gazette 21 6(2014) 1215-1219 .
- [4] Fell, B J. (2009) Structured Mesh Optimisation and CFD Simulation of the Fully Appended DARPA Suboff Model, Australian Maritime Collage, National Center for Maritime Engineering and Hydrodynamics
- [5] Bakker,A. (2006) Lecture 7 - Meshing, Applied Computational Fluid Dynamics , [www.bakker.org](http://www.bakker.org)
- [6] ANSYS Inc. (2013) CFX Solver Theory Guide Release 15 . Southpointe, 275 Technology Drive Canonsburg, PA.
- [7] Mulvany , N. Chen, L. Tu, J. Anderson, B . (2004) Steady-State Evaluation of 'Two-Equation' RANS (Reynolds-averaged Navier-Stokes) Turbulence Models for High-Reynolds Number Hydrodynamic Flow Simulations .Maritime Platforms Division (2004) Australia, DSTO-TR-1564
- [8] Dittrich, R (1972) EXPERIMENTAL STUDY OF FLOW DISTRIBUTION AND PRESSURE LOSS WITH CIRCUMFERENTIAL INLET AND OUTLET MANIFOLDS (1972) NASA, Lewis Research Center
- [9] Lymberopoulos, N. Baines, N. Watson, N. (1988) Flow in Single and Twin Entry Radial Turbine Volute . Gas Turbine and Aeroengine Congress (1988) , Amsterdam, The Netherlands .
- [10] Gu, F . Engeda, A. Benisek, E. (2001) A comparative study of incompressible and compressible design approaches of radial inflow turbine volutes .Proceedings of the Institution of Mechanical Engineers (2001).
- [11] Grönman, A . (2010) Numerical modelling of small supersonic axial flow turbines. Acta Universitatis (2010) Lappeenrantaensis .
- [12] Engine Soft (2008) Meta-modeling with modeFRONTIER: Advantaged and Perspectives , Newsletter EnginSoft - modeFRONTIER Special Issue (2008) .
- [13] ESTECO srl (2008) Response surface methodologies, modeFRONTIER.
- [14] ESTECO (2008) A simple multi-objective optimization problem , modeFRONTIER (2008)





# A

## "How to manual" for generating geometries

Removed due to commercial confidentiality.



# B

## Detailed explanation of the ICEM script

Removed due to commercial confidentiality.



# C

## Test plan

Removed due to commercial confidentiality.



# D

## Boundary condition

Removed due to commercial confidentiality.





# E

## **Results Massflow and static pressure into each stator segment**

Removed due to commercial confidentiality.